Duodenal microbiome in chronic kidney disease

近藤, 雅浩

Duodenal microbiome in chronic kidney disease

Masahiro Kondo (MD)[1], Takehiro Torisu (MD, PhD)[1], Tomohiro Nagasue (MD, PhD)[1], Hiroki Shibata (PhD)[2], Junji Umeno (MD, PhD)[1], Keisuke Kawasaki (MD, PhD)[1], Shin Fujioka (MD, PhD)[1], Yuichi Matsuno (MD, PhD)[1], Tomohiko Moriyama (MD, PhD)[1,3], Takanari Kitazono (MD, PhD)[1]

1) Department of Medicine and Clinical Science, Graduate School of Medical Sciences, Kyushu University, Fukuoka, Japan
2) Medical Institute of Bioregulation, Kyushu University, Fukuoka, Japan
3) International Medical Department, Kyushu University Hospital, Fukuoka, Japan

Correspondence to:

Takehiro Torisu

Department of Medicine and Clinical Science, Graduate School of Medical Sciences, Kyushu University,

Maida-shi 3-1-1, Higashi-ku, Fukuoka 812-8582, Japan

Phone: +81(Japan)-92-642-5261

Fax: +81(Japan)-92-642-5273

E-mail: torisu.takehiro.437@m.kyushu-u.ac.jp

The number of words in the manuscript : 3863

Author contribution Conceptualization

M.K., T.T., T.N., J.U., K.K., S.F., Y.M., and T.M. contributed to the conception and design of this study. M.K., T.N., T.T., and T.K. proofread this manuscript. H.S. was central to the acquisition of the sequence data. All the authors read and approved the final manuscript.

Funding statement This study was supported by JSPS KAKENHI Grant Number JP21K06783, Grant-in-Aid for Scientific Research C.

Declaration of conflict of interest The authors declare that there are no conflicts of interest.

Abstract

Background The intestinal microbiome is involved in the pathogenesis of chronic kidney disease (CKD). Despite its importance, the microbiome of the small intestinal mucosa has been little studied due to sampling difficulties, and previous studies have mainly focused on fecal sources for microbiome studies. We aimed to characterize the small intestinal microbiome of CKD patients by studying the microbiome collected from duodenal and fecal samples of CKD patients and healthy controls.

Methods Overall, 28 stage 5 CKD patients and 21 healthy participants were enrolled. Mucosal samples were collected from the deep duodenum during esophagogastroduodenoscopy and fecal samples were also collected. The 16S ribosomal RNA gene sequencing using Qiime2 was used to investigate and compare the microbial structure and metagenomic function of the duodenal and fecal microbiomes.

Results The duodenal flora of CKD patients had decreased alpha diversity compared with the control group. On the basis of taxonomic composition, Veillonella and Prevotella were significantly reduced in the duodenal flora of CKD patients. The tyrosine and tryptophan metabolic pathways were enhanced in the urea toxin-related metabolic pathways based on the Kyoto Encyclopedia of Genes and Genomes database.

Conclusions The small intestinal microbiome in CKD patients is significantly altered, indicating that increased intestinal permeability and production of uremic toxin may occur in the upper small intestine of CKD patients.

Keywords chronic kidney disease, gut microbiome, duodenal microbiome, metagenomics, pathway analysis

Introduction

Chronic kidney disease (CKD) is a progressive disease characterized by structural and functional changes in the kidneys due to a variety of causes. The number of CKD patients is on the rise worldwide and it is estimated that one to two million people will die from CKD each year, which will make it the fifth leading cause of death worldwide by 2040. Across different countries, 6%–10% of adult men are classified as having various stages of CKD, making this disease a serious global health problem [1].

The gut microbiome plays an important role in the pathogenesis of CKD. The gut microbiome is involved in the production of uremic substances by metabolic modification of amino acids in the gastrointestinal tract. Regarding the formation of uremic substances, indoxyl sulfate is metabolized from tryptophan to indole and p-cresyl sulfate is metabolized from tyrosine to p-cresol by intestinal bacteria [2] [3]. Trimethylamine N-oxide is also produced by the metabolism of choline and L-carnitine to trimethylamine by intestinal bacteria [4]. These uremic toxins disrupt the tight junctions in the intestinal tract [5], facilitating the increase of uremic toxins in the blood circulation. Furthermore, as CKD progresses, uremic

substances tend to accumulate in the body, leading not only to kidney fibrosis [6] but also to uremia and risk of cardiovascular complications [7].

In addition to uremic toxins, dysbiosis of the intestinal microbiome is thought to cause an increase in peptidoglycan and lipopolysaccharide in the intestinal tract due to overgrowth of pathogenic bacteria. These bacterial-derived substances also activate intestinal immunity by increasing intestinal permeability [8], and exacerbate CKD by inducing inflammation through inflammatory cytokines [9]. Thus, the relationship between intestinal bacteria and CKD is considered as "the gut-kidney axis" [10]. .

Most studies investigating the intestinal microbiome in CKD patients have used fecal samples due to the ease of specimen collection; however, recent studies have reported differences in intestinal bacteria among the various parts of the gastrointestinal tract and the feces [11] [12]. Bacterial metabolites also differ between feces and the gastrointestinal mucosa, and uremic toxin have been shown to be more abundant in the small intestinal mucosa [13] [14]. However, the bacterial flora in the small intestine of CKD patients has not been well studied because of the difficulty of obtaining samples and our limited understanding of the characteristics of the small intestinal microbiome. Previous studies have shown that the composition of the duodenal and jejunal flora is similar [11], and we therefore examined the duodenal flora of CKD patients to characterize the microbial population and estimate the bacterial gene function of the small intestinal flora.

Materials and Methods

Subjects

Patients with stage 5 CKD who underwent esophagogastroduodenoscopy (EGD) at Kyushu University Hospital between April 2020 and October 2021 and healthy controls were enrolled in the study. Patients with gastrointestinal malignancies, inflammatory bowel disease, and those who had taken antibiotics or probiotics 3 months prior to EGD were excluded due to the possibility of significant effects on the intestinal microbiome. Patients who were post renal transplant or undergoing dialysis treatment were also excluded. All participants signed an informed consent form. Ultimately, 28 CKD patients and 21 healthy subjects were enrolled. The study was approved by the Ethics Review Committee of the Kyushu University Medical School District Office (Permit No. 2020-332) and was conducted in accordance with the 1964 Declaration of Helsinki.

Sample Collection

The metabolic pathway of tryptophan, which is involved in the metabolism of major uremic toxins, has been shown to be abundant in the duodenum (Supplementary figure1), and therefore duodenal and stool samples were collected. Duodenal samples were collected from the mucosal surface of the descending or horizontal part with a COOK medical endoscopy cytology brush (Cook Medical, Tokyo, Japan) during EGD at approximately 9:00-10:00. The collected samples were stored frozen at −80°C. Fecal samples were

collected either the day before or the day after the EGD. Fecal samples were stored at 2°C in DNA storage solution (Techno Suruga Laboratory, Shizuoka, Japan) until processing.

Bacterial DNA was extracted from the mucosal samples using NucleoSpin® Tissue XS (Macherey-Nagel, Duren, Germany) after homogenization with BEADS CRUSHER μT-12® (TAITEC, Koshigaya, Japan). Fecal bacterial DNA was extracted using the same procedure with NucleoSpin® Tissue (Macherey-Nagel, Duren, Germany).

As described previously, 16S ribosomal RNA (rRNA) gene sequencing was conducted with minor modifications [15].

Bioinformatics and Statistical Analysis

Amplicon sequence quality control was performed using the Divisive Amplicon Denoising Algorithm2 (DADA2) and reads were processed using QIIME2 (ver. 2021.2) [16] .. Representative sequences were classified using the SILVA database (v.138) [17] and by training a naïve Bayes classifier using the q2-feature-classifier plugin.

The alpha diversity was indexed using the α-rarefaction plugin and assessed by the Kruskal–Wallis test. Beta diversity was calculated using the core-metrics-phylogenetic plugin and the Bray–Curtis distance, and these distances were displayed by the non-metric multidimensional scaling (NMDS). The NMDS plots were visualized using the ggplot2 package in R software (https://www.r-project.org/), and each group was surrounded by an ellipse with 95% confidence intervals and anlyzed with a similarity analysis test.

QIIME2 was used to obtain tables of composition and abundance for each sample at two taxonomic levels (phylum and genus). Phylogenetic Investigation of Communities by Reconstruction of Unobserved States plugin (PICRUSt2) [18] was used to predict the functional profile of microbial communities, and the MetaCyc pathway [19] and Kyoto Encyclopedia of Genes and Genomes (KEGG) pathway were normalized within QIIME2. The open-source software STAMP (Statistical Analysis of Metagenomics Profiles) was used to assess the significance of differences in microbial community structure and functional profile predictions between groups and differences were analyzed using Welch's t-test option [20]. Results were considered statistically significant when $p < 0.05$.

RESULTS

Table 1 shows the clinical characteristics of the participants (28 in the CKD group and 21 in the control group). Median age was 68 years in the CKD group and 55 years in the control group. Regarding gender, 28.6% of the patients were female in the CKD group and 57.1% in the control group. No differences were found in BMI, alcohol, smoking, or use of medications such as antithrombotic drugs, proton pump inhibitor (PPI), or steroids. The most common cause of CKD was glomerulonephritis (32.1%), followed by diabetes (28.6%) and hypertension (10.7%). Blood data showed that white blood cell count was higher and

hemoglobin and albumin levels were lower in the CKD group. Not surprisingly, blood urea nitrogen (BUN), creatinine (Cr), estimated glomerular filtration rate (eGFR), and creatinine clearance (Ccr) all revealed significantly lower renal function in the CKD group.

Comparison of alpha and beta diversity

To compare the homogeneity and abundance of the intestinal microbiome within the samples, the Chao1 index, Shannon index, and Simpson index were calculated and compared as a measure of alpha diversity (Figure 1). In the duodenal flora, Chao1 index was significantly lower in the CKD group, and Shannon index and Simpson index also tended to be lower in the CKD group, although no significant differences were observed. There was no difference in alpha diversity of the fecal microbiome between the two groups.

The beta diversity analysis was displayed in an NMDS plot based on the calculation of the Bray–Curtis distance (Figure 2). Both the duodenal and fecal flora revealed that the community composition of the bacterial flora in the CKD group differed from that of the control group.

The duodenal microbiota of CKD patients with diabetes mellitus (DM) (n=8) was compared with that of CKD patients without DM (n=20), and no significant differences were found in both alpha and beta diversity (Supplementary figure 3). When PPI users (CKD group; n=2, control group; n=4) were excluded, the diversity of duodenal microbiota was similar to that of those not excluded (Supplementary figure 4).

Comparison of taxonomic composition

Figure 3 shows the comparison of the taxonomic composition of the duodenal and fecal flora of the CKD and control groups at the phylum level. Firmicutes, Bacteroides, Proteobacteria, and Actinobacteriota, which are the major phylum of human intestinal bacteria, accounted for the majority of bacteria in the CKD group, but the proportions of these bacteria in the duodenal and fecal flora were significantly different (Figure 3a). For the duodenal flora, Proteobacteria were significantly increased in the CKD group, while Firmicutes and Actinobacteriota were significantly decreased in the CKD group (Figure 3b). No significant differences were found in the proportion of major bacterial phylum present in the fecal flora (Figure 3c). Figure 4 compares the taxonomic composition of the bacteria at the genus level. Again, the composition of the duodenal and fecal flora differed significantly. Streptococcus, Veillonella, and Prevotella were abundant in the duodenal flora, while Bacteroides, Bifidobacterium, and Blautia were abundant in the fecal flora (Figure 4a). In the duodenal flora, Veillonella, Prevotella, Rothia, and Megasphaera were decreased and Capnocytophaga was increased in the CKD group compared with the control group (Figure 4b). In the fecal flora, Parabacteroides increased in the CKD group, whereas Fusicatenibacter and Dorea decreased (Figure 4c).

Prediction of bacterial metabolic pathways in CKD

Supplementary figure 2 compares the relative abundance of genes involved in pathways in the CKD and

control groups analyzed by PICRUSTs2. In the duodenal flora, the relative abundance of 120 pathways was significantly altered. Compared with the control group, the relative abundance of 72 pathways was significantly increased and that of 48 pathways was significantly decreased in the CKD group. The 10 pathways with the greatest changes are shown in Figure 5a. Inflammation-inducing bacterial wall components such as peptidoglycan recycling I and factors involved in the synthesis of sulfur-containing amino acids such as superpathway of sulfate assimilation and cysteine biosynthesis and superpathway of L-methionine biosynthesis were significantly increased in the CKD group. In the fecal flora, 39 pathways were significantly altered, and 24 pathways were increased and 16 pathways were decreased in the CKD group compared to the control group. The 10 pathways with the largest changes are shown in Figure 5b. In the fecal flora, peptidoglycan recycling I was also increased in the CKD group.

To investigate the effect of the gut microbiome on uremic toxin, functional composition prediction and annotation of tyrosine and tryptophan metabolism were performed based on the KEGG database. Comparing the duodenal flora of the CKD and control groups, 11 pathways for tyrosine metabolism and four pathways for tryptophan metabolism were significantly altered (Figure 6a). All of these pathways were increased in the CKD group. In the fecal flora, five pathways related to tyrosine metabolism and six pathways related to tryptophan metabolism were significantly altered (Figure 6b). All but one pathway involved in tyrosine metabolism was increased in the CKD group, and all pathways involved in tryptophan metabolism were increased in the CKD group.

Discussion

To the best of our knowledge, this study is the first to investigate the duodenal microbiome in CKD patients. The relationship between CKD and the intestinal microbiome has been intensively studied through analysis of fecal samples, and abnormalities in the fecal microbiome have been implicated in the development and progression of CKD [21]. Comprehensive metabolic maps of the gastrointestinal tract have also shown that metabolites in stool and mucosa are different, and that uremic toxins derived from enterobacteria are abundant in the small intestinal mucosa [13,14]. Little is known about the characteristics of the gastrointestinal mucosal flora in CKD patients, which are thought to contribute to the pathogenesis of CKD, and we believe that this study is significant because it provides a characterization of the duodenal mucosal flora.

Previous studies using fecal material have reported that the diversity, overall richness, and structure of the microbiome are significantly different in CKD patients compared with healthy humans [22] [23]. In this study, analysis of the alpha diversity of the gastrointestinal mucosal flora revealed a significant decrease in Chao1 index in CKD patients, which is consistent with previous reports using fecal samples. Not only bacteria in the stool, but also metabolic products produced by mucosa-associated bacteria in the digestive tract, are absorbed into the host's circulation. Several uremic toxins are reported to be more abundant in the

small intestine mucosa [14]. Furthermore, while stool samples are influenced by the lower digestive tract, duodenal samples reflect the mucosa-associated bacterial community in regions more involved in absorption [11]. The difference in alpha diversity between the CKD and control groups shown in the gastrointestinal mucosal flora in this study was not detected in the fecal flora, suggesting that the gastrointestinal mucosal flora may more sensitively reflect changes in diversity. Analysis of beta diversity also showed that the bacterial flora of CKD patients and healthy humans form different communities in the gastrointestinal tract.

In the gastrointestinal mucosal flora of CKD patients, Proteobacteria were increased among the major phylum and the proportion of Firmicutes and Actinobacteriota was decreased. Proteobacteria are anaerobic bacteria that comprise a small percentage of the intestinal microbiome in healthy humans, but have been found to increase in dysbiosis, and an increase in Proteobacteria often coincides with a deterioration of the intestinal microbiome structure and inflammation [24]. The characteristics of the gastrointestinal mucosal flora in patients with CKD may suggest dysbiosis.

In this study, Veillonella and Prevotella were also noticeably decreased in the gastrointestinal mucosal flora of CKD patients. Veillonella is also decreased in saliva and oral cavity of CKD patients [25], and Veillonella in feces has been shown to be negatively correlated with p-cresyl sulfate [26]. It has been suggested that the decrease in Veillonella may play an important role in the progression of CKD, and the results of this study support this theory. Prevotella has also been reported to be decreased in CKD patients in studies using fecal samples [27]. Prevotella in feces is also reported to be negatively correlated with the uremic toxin TMAO and p-cresylglucuronic acid [26], and a decrease in Prevotella in the gastrointestinal mucosal flora of CKD patients may affect the production and absorption of uremic toxin. Prevotella is a butyrate-producing bacterium, and butyrate plays a role in regulating inflammation in the body by controlling Treg cell differentiation [28]. The role of the small intestine in immunity is important, and a decrease in Prevotella in the upper small intestinal flora is an important change, which may contribute to CKD. While it is not clear whether replenishing these depleted bacterial species becomes a treatment for CKD, Recent study showed that Bacteroides play an important role in tryptophan metabolism and altering Bacteroides can modulate circulating uremic toxin [29]. In CKD patients, there have been reports of microbiota modulation through nutritional therapy contributing to CKD management [30]. Future treatment strategies targeting the microbiota are also anticipated.

In this study, both gastrointestinal mucosal and fecal bacterial flora suggested an enhanced predicted function of the Peptidoglycan recycling I pathway in the CKD group. Peptidoglycans are components of bacterial cell walls and cause inflammation in the host organism. Peptidoglycans can cross the intestinal epithelial barrier under conditions of increased intestinal permeability, such as CKD, and activate the Hypothalamic-Pituitary-Adrenal (HPA) axis via activation of the immune system [31]. Activation of the HPA axis has been reported to be associated with the prevalence of CKD in patients with type 2 diabetes [32].

The amino acids, tyrosine and tryptophan, ingested from the diet are metabolized by the gut microbiome into p-cresol and indole, which are then absorbed from the gut into the blood and metabolized in the liver into the uremic toxins p-cresyl sulfate and indoxyl sulfate [33] [34]. Precursors of enterobacteria-derived uremic toxins, including p-cresol and indole have reported that their absorption is an event that occurs in the small intestine [13] [14]. Although the density of the gut microbiome in the small intestine is lower than in the large intestine, the different composition of the small and large intestinal microbiome may be associated with different metabolic functions and have different effects on the host. In the present study, the finding that changes in predicted KEGG function related to tyrosine and tryptophan metabolism in the duodenal microbiome were, for the most part, abundant in CKD patients indicates that the production of these uremic toxins occurs not only in the colon but also in the small intestine, where they may be absorbed and enter the systemic circulation, possibly contributing to the exacerbation of CKD.

Our study had several limitations. First, the sample size was not sufficient because the study was conducted at a single institution. The gut microbiota is known to be relatively stable in the long term [35], but exhibits diural oscillations have also been reported [36]. Therefore, we employed a consistent collection protocol to the best extent possible. However, the sample collection during EGD is slightly invasive and not frequently performed making more difficult to collect the duodenal samples compared with fecal samples in other studies, which are easier and less invasive to collect. CKD patients experience various complications, with DM being the most common underlying condition known to impact the gut microbiota [37]. However, in this study, no significant difference was observed in the comparison between DM and non-DM individuals. Additionally, CKD patients often take multiple medications, which can also significantly influence the gut microbiota. Even when excluding PPI [37], our results were similar. Nevertheless, within the sample size of this study, we were unable to determine the extent to which factors other than renal function affect the gut microbiota. The association between gut microbiome and functional pathways of CKD were analyzed by PICRUSTt2 and did not measure p-cresol and indole in the serum. In animal experiments, modulation of bacteria has successfully reduced circulating uremic toxin levels [29], indicating a causal relationship. However, the impact of the gut microbiota on CKD in humans needs to be investigated metabolites in small intestine and the circulation.

In conclusion, we investigated the duodenal microbiome of CKD patients and found that the intestinal microbiome is significantly altered compared with healthy volunteers. The changes in the small intestinal microbiome that were observed in this study may contribute to increased intestinal permeability and production of uremic toxin in the upper small intestine, which may be an exacerbating factor in CKD. When investigating the relationship between CKD and the intestinal microbiome, analysis of the mucosal microbiome of the duodenum and other sections of the gastrointestinal tract may provide new insights that cannot be detected by analysis of the fecal microbiome.

Declarations

Ethics Approval

All procedures performed in studies involving human participants were in accordance with the ethical standards of the institutional and/or national research committee and with the 1964 Helsinki Declaration and its later amendments or comparable ethical standards. The study was approved by the Bioethics Committee of the Kyushu University Medical School District Office (Permit No. 2020-332).

Author Contributions

Acknowledgments

We thank Wendy Hempstock, PhD, from Edanz (https://jp.edanz.com/ac) for editing a draft of this manuscript.

References

1 Jha V, Garcia-Garcia G, Iseki Ket al. . Chronic kidney disease: global dimension and perspectives *Lancet*. 2013;382:260-272.

2 Agus A, Planchais J, Sokol H. Gut Microbiota Regulation of Tryptophan Metabolism in Health and Disease *Cell Host Microbe*. 2018;23:716-724.

3 Mishima E, Fukuda S, Mukawa Cet al. . Evaluation of the impact of gut microbiota on uremic solute accumulation by a CE-TOFMS-based metabolomics approach *Kidney Int*. 2017;92:634-645.

4 Koeth RA, Wang Z, Levison BSet al. . Intestinal microbiota metabolism of L-carnitine, a nutrient in red meat, promotes atherosclerosis *Nat Med*. 2013;19:576-585.

5 Vaziri ND, Yuan J, Rahimi A, Ni Z, Said H, Subramanian VS. Disintegration of colonic epithelial tight junction in uremia: a likely cause of CKD-associated inflammation *Nephrol Dial Transplant*. 2012;27:2686-2693.

6 Sun CY, Chang SC, Wu MS. Uremic toxins induce kidney fibrosis by activating intrarenal renin-angiotensin-aldosterone system associated epithelial-to-mesenchymal transition *PLoS One*. 2012;7:e34026.

7 Vanholder R, Schepers E, Pletinck A, Nagler EV, Glorieux G. The uremic toxicity of indoxyl sulfate and p-cresyl sulfate: a systematic review *J Am Soc Nephrol*. 2014;25:1897-1907.

8 Sabatino A, Regolisti G, Brusasco I, Cabassi A, Morabito S, Fiaccadori E. Alterations of intestinal barrier and microbiota in chronic kidney disease *Nephrol Dial Transplant*. 2015;30:924-933.

9 Darisipudi MN, Knauf F. An update on the role of the inflammasomes in the pathogenesis

of kidney diseases *Pediatr Nephrol*. 2016;31:535-544.

10 Meijers BK, Evenepoel P. The gut-kidney axis: indoxyl sulfate, p-cresyl sulfate and CKD progression *Nephrol Dial Transplant*. 2011;26:759-761.

11 Nagasue T, Hirano A, Torisu Tet al. . The Compositional Structure of the Small Intestinal Microbial Community via Balloon-Assisted Enteroscopy *Digestion*. 2022;103:308-318.

12 Leite GGS, Weitsman S, Parodi Get al. . Mapping the Segmental Microbiomes in the Human Small Bowel in Comparison with Stool: A REIMAGINE Study *Dig Dis Sci*. 2020;65:2595-2604.

13 Stremmel W, Schmidt KV, Schuhmann Vet al. . Blood Trimethylamine-N-Oxide Originates from Microbiota Mediated Breakdown of Phosphatidylcholine and Absorption from Small Intestine *PLoS One*. 2017;12:e0170742.

14 Meier KHU, Trouillon J, Li Het al. . Metabolic landscape of the male mouse gut identifies different niches determined by microbial activities *Nat Metab*. 2023.

15 Hirano A, Umeno J, Okamoto Yet al. . Comparison of the microbial community structure between inflamed and non-inflamed sites in patients with ulcerative colitis *J Gastroenterol Hepatol*. 2018.

16 Bolyen E, Rideout JR, Dillon MRet al. . Reproducible, interactive, scalable and extensible microbiome data science using QIIME 2 *Nat Biotechnol*. 2019;37:852-857.

17 Quast C, Pruesse E, Yilmaz Pet al. . The SILVA ribosomal RNA gene database project: improved data processing and web-based tools *Nucleic Acids Res*. 2013;41:D590-596.

18 Douglas GM, Maffei VJ, Zaneveld JRet al. . PICRUSt2 for prediction of metagenome functions *Nat Biotechnol*. 2020;38:685-688.

19 Caspi R, Billington R, Keseler IMet al. . The MetaCyc database of metabolic pathways and enzymes - a 2019 update *Nucleic Acids Res*. 2020;48:D445-d453.

20 Parks DH, Tyson GW, Hugenholtz P, Beiko RG. STAMP: statistical analysis of taxonomic and functional profiles *Bioinformatics*. 2014;30:3123-3124.

21 Hobby GP, Karaduta O, Dusio GF, Singh M, Zybailov BL, Arthur JM. Chronic kidney disease and the gut microbiome *Am J Physiol Renal Physiol*. 2019;316:F1211-f1217.

22 Li F, Wang M, Wang J, Li R, Zhang Y. Alterations to the Gut Microbiota and Their Correlation With Inflammatory Factors in Chronic Kidney Disease *Front Cell Infect Microbiol*. 2019;9:206.

23 Wu IW, Gao SS, Chou HCet al. . Integrative metagenomic and metabolomic analyses reveal severity-specific signatures of gut microbiota in chronic kidney disease *Theranostics*. 2020;10:5398-5411.

24 Shin NR, Whon TW, Bae JW. Proteobacteria: microbial signature of dysbiosis in gut microbiota *Trends Biotechnol*. 2015;33:496-503.

25 Hu J, Iragavarapu S, Nadkarni GNet al. . Location-Specific Oral Microbiome Possesses Features Associated With CKD *Kidney Int Rep*. 2018;3:193-204.

26 Kim JE, Kim HE, Park JIet al. . The Association between Gut Microbiota and Uremia of Chronic Kidney Disease *Microorganisms*. 2020;8.

27 Jiang S, Xie S, Lv Det al. . Alteration of the gut microbiota in Chinese population with chronic kidney disease *Sci Rep*. 2017;7:2870.

28 Furusawa Y, Obata Y, Fukuda Set al. . Commensal microbe-derived butyrate induces the differentiation of colonic regulatory T cells *Nature*. 2013;504:446-450.

29 Devlin AS, Marcobal A, Dodd Det al. . Modulation of a Circulating Uremic Solute via Rational Genetic Manipulation of the Gut Microbiota *Cell Host Microbe*. 2016;20:709-715.

30 Di Iorio BR, Rocchetti MT, De Angelis Met al. . Nutritional Therapy Modulates Intestinal Microbiota and Reduces Serum Levels of Total and Free Indoxyl Sulfate and P-Cresyl Sulfate in Chronic Kidney Disease (Medika Study) *J Clin Med*. 2019;8.

31 Wheeler R, Bastos PAD, Disson Oet al. . Microbiota-induced active translocation of peptidoglycan across the intestinal barrier dictates its within-host dissemination *Proc Natl Acad Sci U S A*. 2023;120:e2209936120.

32 Asao T, Oki K, Yoneda M, Tanaka J, Kohno N. Hypothalamic-pituitary-adrenal axis activity is associated with the prevalence of chronic kidney disease in diabetic patients *Endocr J*. 2016;63:119-126.

33 Banoglu E, Jha GG, King RS. Hepatic microsomal metabolism of indole to indoxyl, a precursor of indoxyl sulfate *Eur J Drug Metab Pharmacokinet*. 2001;26:235-240.

34 Wang X, Yang S, Li Set al. . Aberrant gut microbiota alters host metabolome and impacts renal failure in humans and rodents *Gut*. 2020;69:2131-2142.

35 Thaiss CA, Zeevi D, Levy Met al. . Transkingdom control of microbiota diurnal oscillations promotes metabolic homeostasis *Cell*. 2014;159:514-529.

36 Faith JJ, Guruge JL, Charbonneau Met al. . The long-term stability of the human gut microbiota *Science*. 2013;341:1237439.

37 Nagata N, Nishijima S, Miyoshi-Akiyama Tet al. . Population-level Metagenomics Uncovers Distinct Effects of Multiple Medications on the Human Gut Microbiome *Gastroenterology*. 2022;163:1038-1052.

Table 1. Characteristics of participants.

	CKD (n=28)	Control (n=21)	p-value
Age	60.5±15.7	58.6±16.7	0.688
Gender(female)	8 (28.6%)	12 (57.1%)	0.077
BMI	22.9±4.1	22.7±4.2	0.877
Alcohol	4 (14.3%)	4 (19.1%)	0.71
Smoking	3 (10.7%)	3 (14.3%)	1
Antithrombotic agent	7 (25%)	2 (9.5%)	0.267
PPI / P-CAB	2 (7.1%)	4 (19.1%)	0.381
Steroid	2 (7.1%)	0	0.5
Helicobactor pylori	4 (14.3%)	6 (28.6%)	0.275
Cause of chronic kidney disease			
Glomerulonephritis	9 (32.1%)	-	
Diabetes	8 (28.6%)	-	
Hypertension	3 (10.7%)	-	
Polycystic kidney disease	2 (7.1%)	-	
Other	6 (21.4%)	-	
WBC(×103/μL)	6.59±2.9	5.2±1.65	0.028
Hb(g/dL)	9.87±1.41	13.5±1.77	<0.001
Plt(×104/μL)	20.99±8.03	22.78±5.34	0.381
TP(mg/dL)	6.21±0.81	6.57±0.59	0.088
Alb(mg/dL)	3.41±0.72	3.99±0.46	0.003
BUN(mg/dL)	65.5±15.94	14.33±5.88	<0.001
Cr(mg/dL)	6.74±2.51	0.64±0.11	<0.001
e-GFR(mL/min/1.73m2)	7.83±2.79	84.6±21.94	<0.001
Ccr(mL/min)	10.42±4.13	90.18±34.18	<0.001
CRP(mg/dL)	0.3±0.41	0.11±0.18	0.051
Glu(mg/dL)	111.32±44.11	90.81±34.99	0.086
TC(mg/dL)	177.57±46	189.14±35.95	0.35
TG(mg/dL)	134.64±65.62	119.05±74.36	0.441
HbA1c(%)	5.78±0.89	5.63±0.22	0.482

Data are presented as mean (± standard deviation) or number (%)

CKD chronic kidney disease, *BMI* body mass index, *PPI* proton pump inhibitor, *P-CAB* potassium

competitive acid blocker, *WBC* white blood cell, *Hb* hemoglobin, *Plt* platelet, *TP* total protein, *Alb* albumin, *BUN* blood urea nitrogen, *Cr* creatinine, *e-GFR* estimated glomerular filtration rate, *Ccr* creatinine clearance, *CRP* C-reactive protein, *Glu* glucose, *TC* total cholesterol, *TG* triglyceride, *HbA1c* hemoglobin A1c

Figure Legends

Figure1 Alpha diversity comparisons by groups
Alpha diversity of duodenal and fecal microbiome in patients with chronic kidney disease (CKD) and healthy control subjects. Comparison of duodenal (a) and fecal (b) microbial diversity, as estimated by the Chao1 index and Shannon index and Simpson index.

Figure2 Beta diversity comparisons by groups
Beta diversity of duodenal and fecal microbiome in patients with chronic kidney disease (CKD) and healthy control subjects.
NMDS (non-metric multidimensional scaling) analysis results based on Bray–Curtis distances of the duodenal (a) and fecal (b) microbiome. CKD and control subjects are denoted with red and blue symbols, the ellipses indicate 95% confidence intervals, respectively.

Figure3 Comparison of the composition of the duodenal and fecal flora at the phylum level in the chronic kidney disease (CKD) and control groups
The bar plots show the comparison of the microbiome's relative abundance at the level of phylum between CKD and control groups, respectively (a). Relative changes of duodenal (b) or fecal (c) bacterial taxa at the Phylum level in the CKD and control groups.

Figure4 Comparison of the composition of the duodenal and fecal flora at the genus level in the chronic kidney disease (CKD) and control groups
The bar plots show the comparison of the microbiome's relative abundance at the level of genus between CKD and control groups, respectively (a). Relative changes of duodenal (b) or fecal (c) bacterial taxa at the genus level in the CKD and control groups.

Figure5 Histogram of the 10 most different pathways determined by Statistical Analysis of Metagenomics

Profiles (STAMP) analysis

(a) STAMP analysis between chronic kidney disease (CKD) and control groups in duodenal flora. (b) Stamp analysis between CKD and control groups in fecal flora.

Figure6 Histograms of Kyoto Encyclopedia of Genes and Genomes (KEGG) pathway abundance and stamp analysis in tyrosine and tryptophan metabolism

(a) Statistical Analysis of Metagenomics Profiles (STAMP) analysis of tyrosine metabolism between CKD and control groups in duodenal microflora. (b) STAMP analysis of tryptophan metabolism between CKD and control groups in duodenal microflora. (c) STAMP analysis of tyrosine metabolism between CKD and control groups in fecal microflora. (d) STAMP analysis of tryptophan metabolism between CKD and control groups in fecal microflora.

Supplementary figure1 Comparison of the predictive functional profiles of microbial communities

Proportion of genes involved in tryptophan metabolic pathways.

Supplementary figure2 Histogram of differing pathway abundances and Statistical Analysis of Metagenomics Profiles (STAMP) analysis

(a) STAMP analysis between CKD and control groups in duodenal flora. (b) STAMP analysis between CKD and control groups in fecal flora.

Supplementary figure3 Alpha and beta diversity comparisons (DM-CKD vs nonDM-CKD)

(a) Alpha diversity of duodenal microbiota in chronic kidney disease (CKD) patients with and without DM. (b) Qualitative measurement of the dissimilarity (Bray-Curtis distance) of the microbial community of CKD patients with DM and CKD patients without DM. In the Principal Coordinate Analysis (PCoA) generated by EMPeror, CKD patients with DM are shown in red and CKD patients without DM in blue.

Supplementary figure4 Alpha and beta diversity comparisons (excluded PPI users).

(a) Alpha diversity of the duodenal microbiota in patients with chronic kidney disease (CKD) and healthy controls when PPI adherents are excluded. (b) Qualitative measurement of the dissimilarity of the microbial community (Bray-Curtis distance) between CKD and controls when PPI adherents are excluded. In the Principal Coordinate Analysis (PCoA) produced by EMPeror, individuals with CKD are shown in red and controls in blue.

a

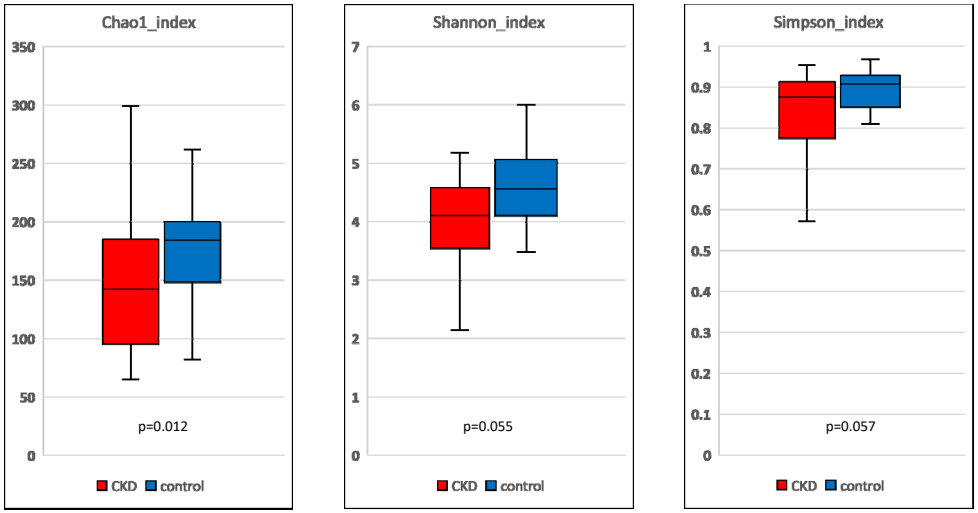
Chao1_index
350
300
250
200
150
100
50
0
p=0.012
CKD
control
Shannon_index
7
6
5
4
3
2
1
0
p=0.055
CKD
control
Simpson_index
1
0.9
0.8
0.7
0.6
0.5
0.4
0.3
0.2
0.1
0
p=0.057
CKD
control

b

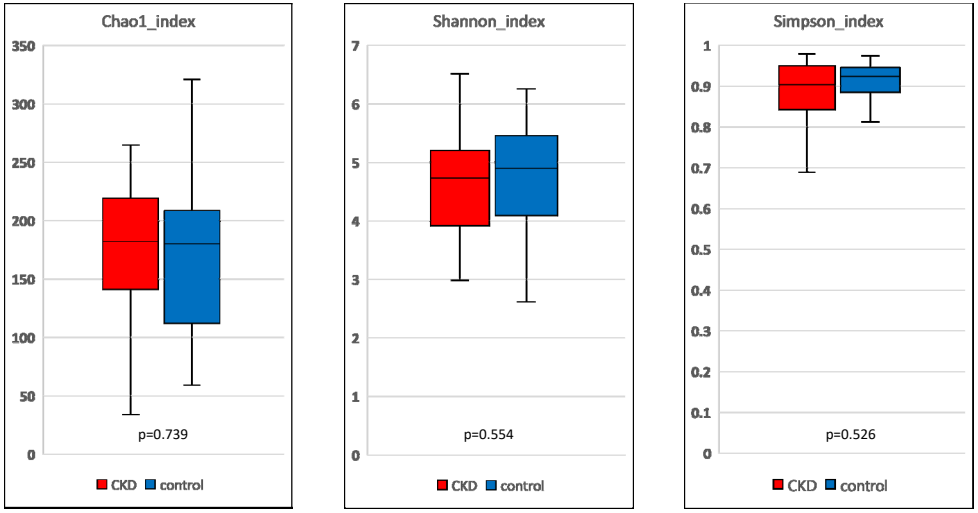
Chao1_index
350
300
250
200
150
100
50
0
p=0.739
CKD
control
Shannon_index
7
6
5
4
3
2
1
0
p=0.554
CKD
control
Simpson_index
1
0.9
0.8
0.7
0.6
0.5
0.4
0.3
0.2
0.1
0
p=0.526
CKD
control

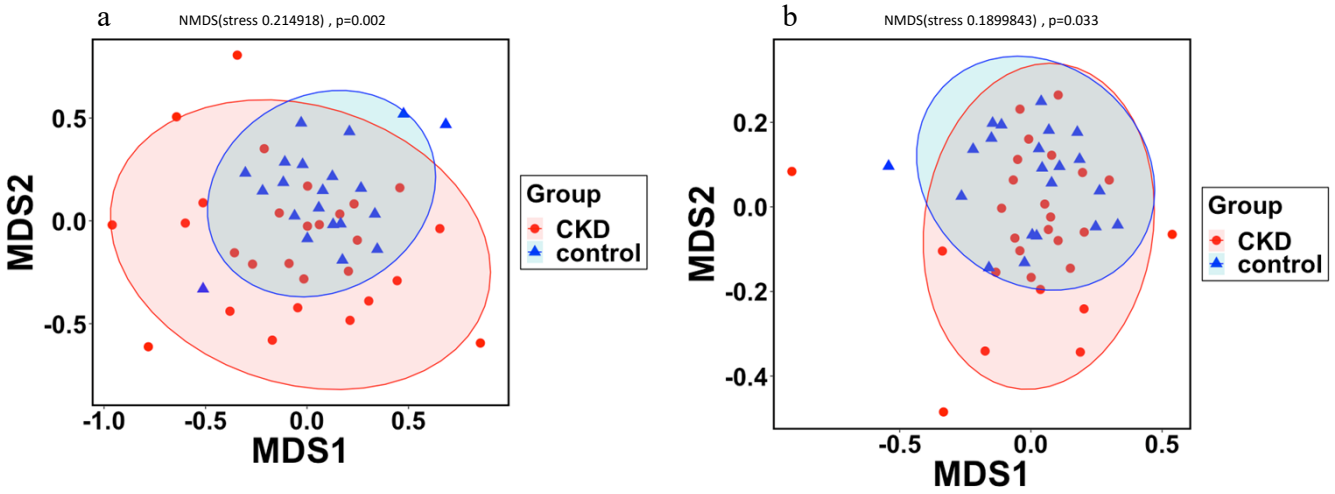
a
NMDS(stress 0.214918) , p=0.002
MDS2
MDS1
0.5
0.0
-0.5
-1.0
-0.5
0.0
0.5
Group
CKD
control
b
NMDS(stress 0.1899843) , p=0.033
MDS2
MDS1
0.2
0.0
-0.2
-0.4
-0.5
0.0
0.5
Group
CKD
control

a

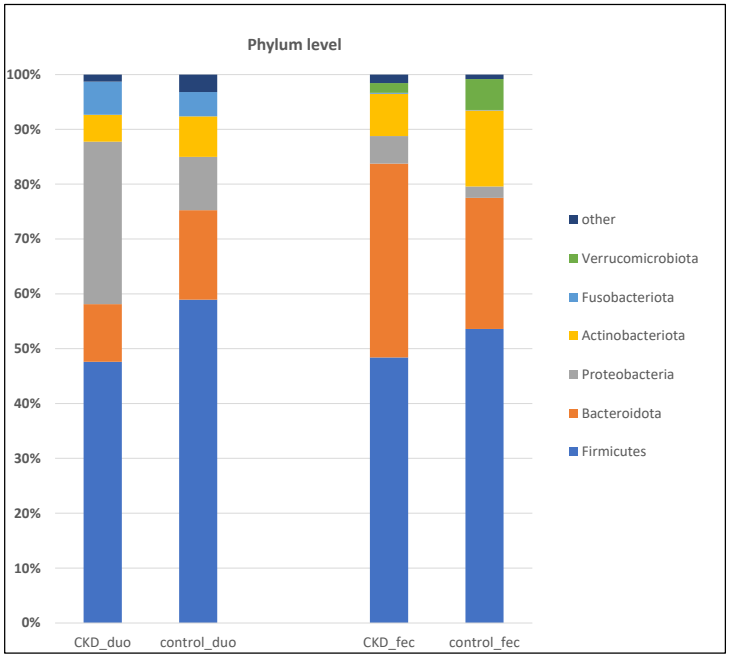
Phylum level
100%
90%
80%
70%
60%
50%
40%
30%
20%
10%
0%
CKD_duo
control_duo
CKD_fec
control_fec
other
Verrucomicrobiota
Fusobacteriota
Actinobacteriota
Proteobacteria
Bacteroidota
Firmicutes

b

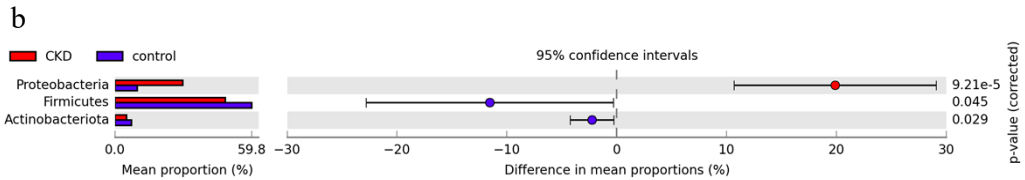
CKD
control
95% confidence intervals
Proteobacteria
Firmicutes
Actinobacteriota
9.21e-5
0.045
0.029
p-value (corrected)
0.0
59.8
Mean proportion (%)
−30
−20
−10
0
10
20
30
Difference in mean proportions (%)

c

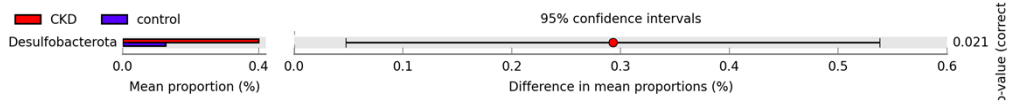
CKD
control
95% confidence intervals
Desulfobacterota
0.021
0.0
0.4
Mean proportion (%)
0.0
0.1
0.2
0.3
0.4
0.5
0.6
Difference in mean proportions (%)

a

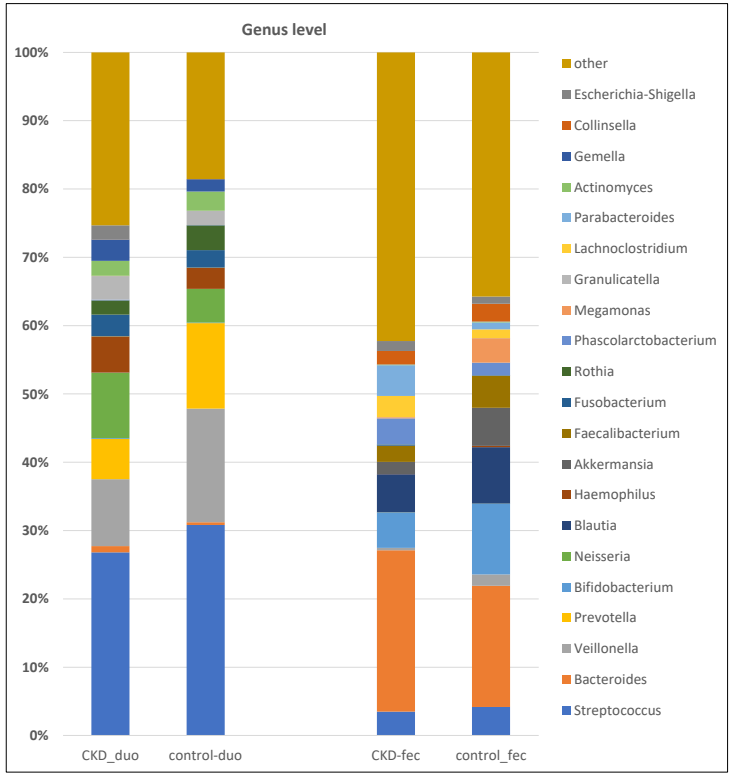
Genus level
100%
90%
80%
70%
60%
50%
40%
30%
20%
10%
0%
CKD_duo
control-duo
CKD-fec
control_fec
other
Escherichia-Shigella
Collinsella
Gemella
Actinomyces
Parabacteroides
Lachnoclostridium
Granulicatella
Megamonas
Phascolarctobacterium
Rothia
Fusobacterium
Faecalibacterium
Akkermansia
Haemophilus
Blautia
Neisseria
Bifidobacterium
Prevotella
Veillonella
Bacteroides
Streptococcus

b

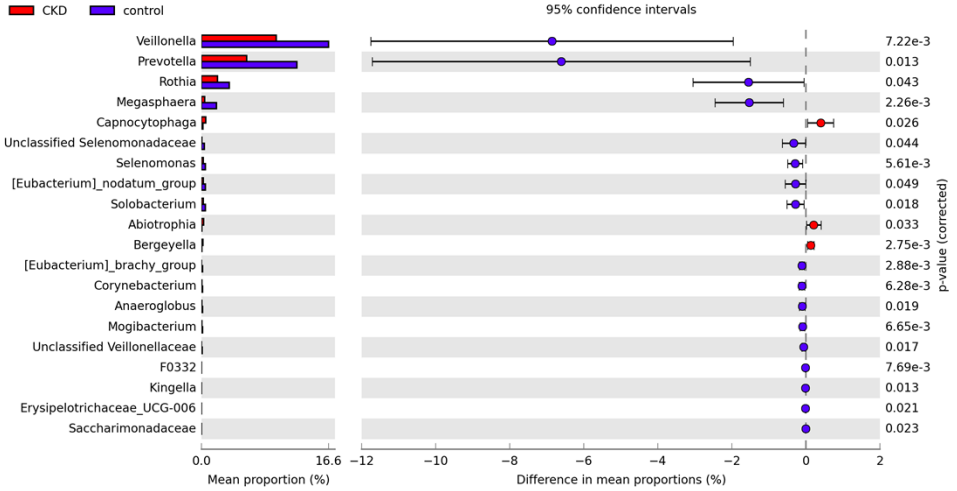
CKD
control
95% confidence intervals
Veillonella 7.22e-3
Prevotella 0.013
Rothia 0.043
Megasphaera 2.26e-3
Capnocytophaga 0.026
Unclassified Selenomonadaceae 0.044
Selenomonas 5.61e-3
[Eubacterium]_nodatum_group 0.049
Solobacterium 0.018
Abiotrophia 0.033
Bergeyella 2.75e-3
[Eubacterium]_brachy_group 2.88e-3
Corynebacterium 6.28e-3
Anaeroglobus 0.019
Mogibacterium 6.65e-3
Unclassified Veillonellaceae 0.017
F0332 7.69e-3
Kingella 0.013
Erysipelotrichaceae_UCG-006 0.021
Saccharimonadaceae 0.023
p-value (corrected)
0.0
16.6
Mean proportion (%)
−12
−10
−8
−6
−4
−2
0
2
Difference in mean proportions (%)

c

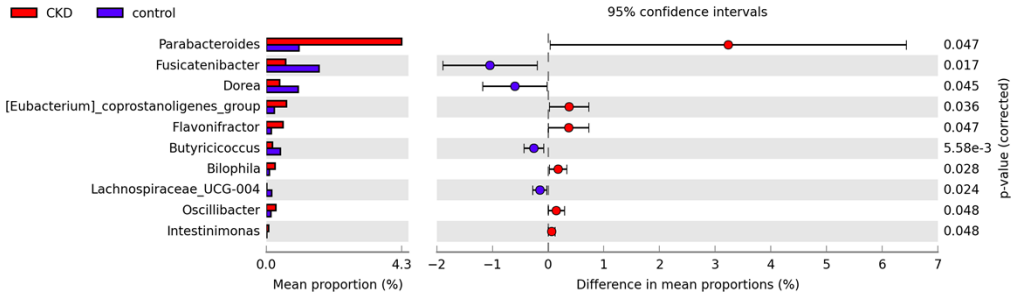
CKD
control
95% confidence intervals
Parabacteroides 0.047
Fusicatenibacter 0.017
Dorea 0.045
[Eubacterium]_coprostanoligenes_group 0.036
Flavonifractor 0.047
Butyricicoccus 5.58e-3
Bilophila 0.028
Lachnospiraceae_UCG-004 0.024
Oscillibacter 0.048
Intestinimonas 0.048
p-value (corrected)
0.0
4.3
Mean proportion (%)
−2
−1
0
1
2
3
4
5
6
7
Difference in mean proportions (%)

a

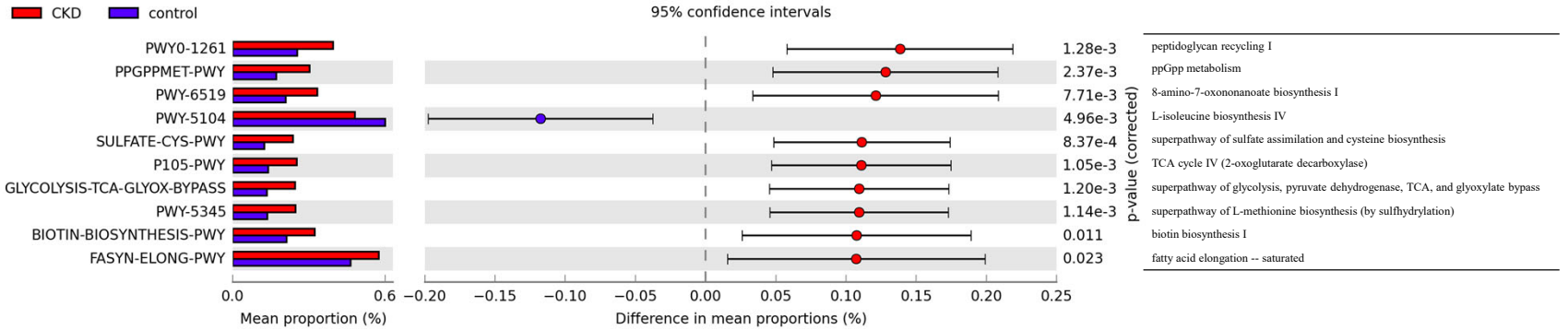
CKD
control
95% confidence intervals
PWY0-1261
PPGPPMET-PWY
PWY-6519
PWY-5104
SULFATE-CYS-PWY
P105-PWY
GLYCOLYSIS-TCA-GLYOX-BYPASS
PWY-5345
BIOTIN-BIOSYNTHESIS-PWY
FASYN-ELONG-PWY
1.28e-3
2.37e-3
7.71e-3
4.96e-3
8.37e-4
1.05e-3
1.20e-3
1.14e-3
0.011
0.023
p-value (corrected)
peptidoglycan recycling I
ppGpp metabolism
8-amino-7-oxononanoate biosynthesis I
L-isoleucine biosynthesis IV
superpathway of sulfate assimilation and cysteine biosynthesis
TCA cycle IV (2-oxoglutarate decarboxylase)
superpathway of glycolysis, pyruvate dehydrogenase, TCA, and glyoxylate bypass
superpathway of L-methionine biosynthesis (by sulfhydrylation)
biotin biosynthesis I
fatty acid elongation -- saturated
0.0
0.6
Mean proportion (%)
−0.20
−0.15
−0.10
−0.05
0.00
0.05
0.10
0.15
0.20
0.25
Difference in mean proportions (%)

b

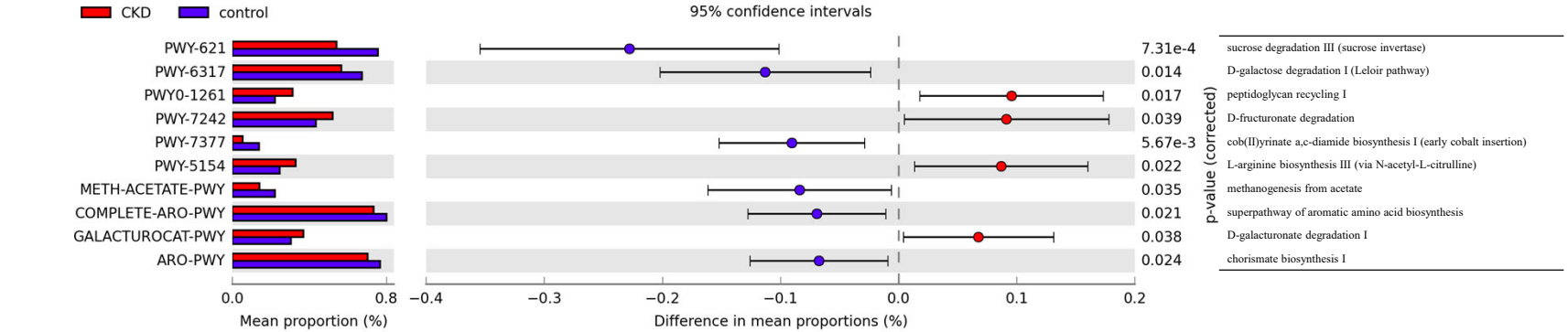
CKD
control
95% confidence intervals
PWY-621
PWY-6317
PWY0-1261
PWY-7242
PWY-7377
PWY-5154
METH-ACETATE-PWY
COMPLETE-ARO-PWY
GALACTUROCAT-PWY
ARO-PWY
7.31e-4
0.014
0.017
0.039
5.67e-3
0.022
0.035
0.021
0.038
0.024
p-value (corrected)
sucrose degradation III (sucrose invertase)
D-galactose degradation I (Leloir pathway)
peptidoglycan recycling I
D-fructuronate degradation
cob(II)yrinate a,c-diamide biosynthesis I (early cobalt insertion)
L-arginine biosynthesis III (via N-acetyl-L-citrulline)
methanogenesis from acetate
superpathway of aromatic amino acid biosynthesis
D-galacturonate degradation I
chorismate biosynthesis I
0.0
0.8
Mean proportion (%)
−0.4
−0.3
−0.2
−0.1
0.0
0.1
0.2
Difference in mean proportions (%)

a

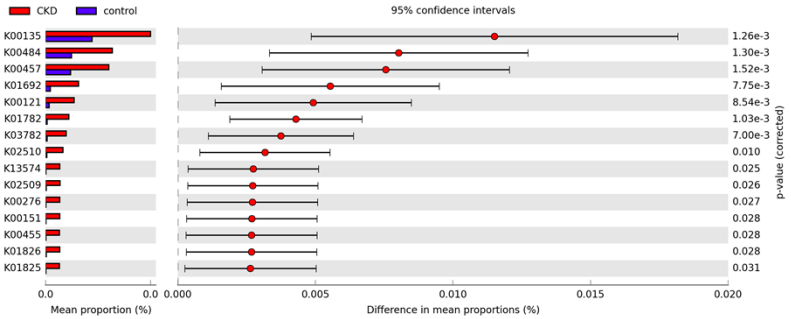
CKD
control
95% confidence intervals
K00135
K00484
K00457
K01692
K00121
K01782
K03782
K02510
K13574
K02509
K00276
K00151
K00455
K01826
K01825
1.26e-3
1.30e-3
1.52e-3
7.75e-3
8.54e-3
1.03e-3
7.00e-3
0.010
0.025
0.026
0.027
0.028
0.028
0.028
0.031
p-value (corrected)
0.0
0.0
0.000
0.005
0.010
0.015
0.020
Mean proportion (%)
Difference in mean proportions (%)

b

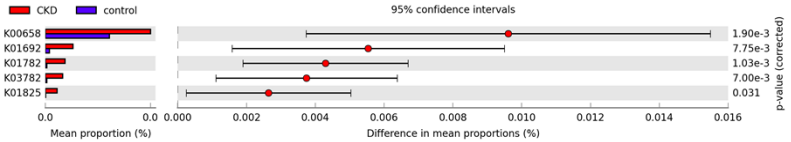
CKD
control
95% confidence intervals
K00658
K01692
K01782
K03782
K01825
1.90e-3
7.75e-3
1.03e-3
7.00e-3
0.031
p-value (corrected)
0.0
0.0
0.000
0.002
0.004
0.006
0.008
0.010
0.012
0.014
0.016
Mean proportion (%)
Difference in mean proportions (%)

c

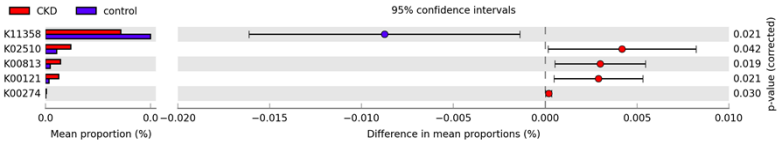
CKD
control
95% confidence intervals
K11358
K02510
K00813
K00121
K00274
0.021
0.042
0.019
0.021
0.030
p-value (corrected)
0.0
0.0
−0.020
−0.015
−0.010
−0.005
0.000
0.005
0.010
Mean proportion (%)
Difference in mean proportions (%)

d

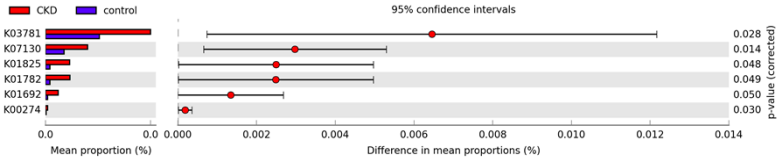
CKD
control
95% confidence intervals
K03781
K07130
K01825
K01782
K01692
K00274
0.028
0.014
0.048
0.049
0.050
0.030
p-value (corrected)
0.0
0.0
0.000
0.002
0.004
0.006
0.008
0.010
0.012
0.014
Mean proportion (%)
Difference in mean proportions (%)

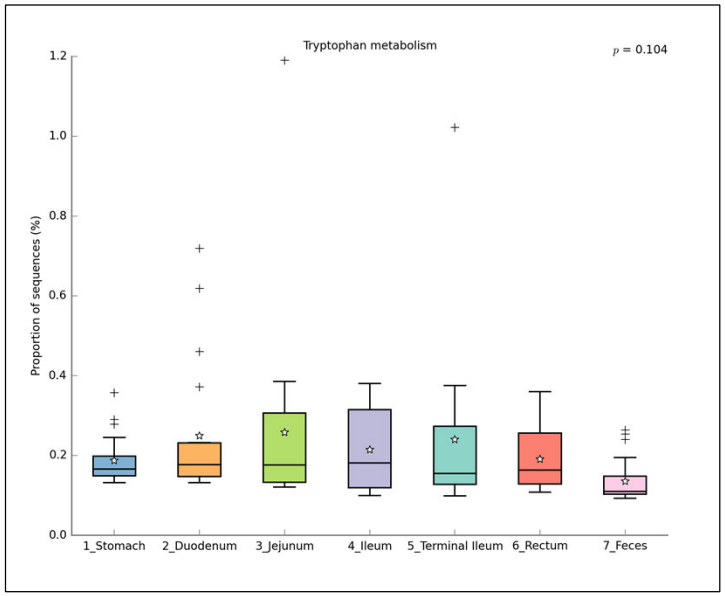
Tryptophan metabolism
p = 0.104
Proportion of sequences (%)
1.2
1.0
0.8
0.6
0.4
0.2
0.0
1_Stomach
2_Duodenum
3_Jejunum
4_Ileum
5_Terminal Ileum
6_Rectum
7_Feces

a

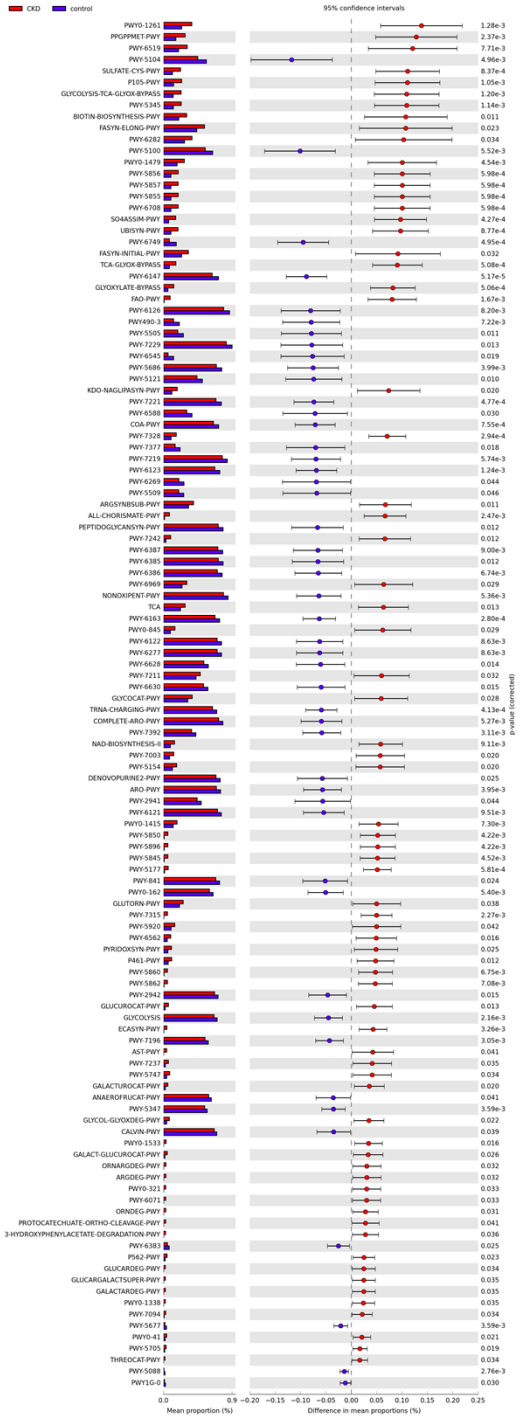
CKD
control
95% confidence intervals
PWY0-1261 1.28e-3
PPGPPMET-PWY 2.37e-3
PWY-6519 7.71e-3
PWY-5104 4.96e-3
SULFATE-CYS-PWY 8.37e-4
P105-PWY 1.05e-3
GLYCOLYSIS-TCA-GLYOX-BYPASS 1.20e-3
PWY-5345 1.14e-3
BIOTIN-BIOSYNTHESIS-PWY 0.011
FASYN-ELONG-PWY 0.023
PWY-6282 0.034
PWY-5100 5.52e-3
PWY0-1479 4.54e-3
PWY-5856 5.98e-4
PWY-5857 5.98e-4
PWY-5855 5.98e-4
PWY-6708 5.98e-4
SO4ASSIM-PWY 4.27e-4
UBISYN-PWY 8.77e-4
PWY-6749 4.95e-4
FASYN-INITIAL-PWY 0.032
TCA-GLYOX-BYPASS 5.08e-4
PWY-6147 5.17e-5
GLYOXYLATE-BYPASS 5.06e-4
FAO-PWY 1.67e-3
PWY-6126 8.20e-3
PWY490-3 7.22e-3
PWY-5505 0.011
PWY-7229 0.013
PWY-6545 0.019
PWY-5686 3.99e-3
PWY-5121 0.010
KDO-NAGLIPASYN-PWY 0.020
PWY-7221 4.77e-4
PWY-6588 0.030
COA-PWY 7.55e-4
PWY-7328 2.94e-4
PWY-7377 0.018
PWY-7219 5.74e-3
PWY-6123 1.24e-3
PWY-6269 0.044
PWY-5509 0.046
ARGSYNBSUB-PWY 0.011
ALL-CHORISMATE-PWY 2.47e-3
PEPTIDOGLYCANSYN-PWY 0.012
PWY-7242 0.012
PWY-6387 9.00e-3
PWY-6385 0.012
PWY-6386 6.74e-3
PWY-6969 0.029
NONOXIPENT-PWY 5.36e-3
TCA 0.013
PWY-6163 2.80e-4
PWY0-845 0.029
PWY-6122 8.63e-3
PWY-6277 8.63e-3
PWY-6628 0.014
PWY-7211 0.032
PWY-6630 0.015
GLYCOCAT-PWY 0.028
TRNA-CHARGING-PWY 4.13e-4
COMPLETE-ARO-PWY 5.27e-3
PWY-7392 3.11e-3
NAD-BIOSYNTHESIS-II 9.11e-3
PWY-7003 0.020
PWY-5154 0.020
DENOVOPURINE2-PWY 0.025
ARO-PWY 3.95e-3
PWY-2941 0.044
PWY-6121 9.51e-3
PWY0-1415 7.30e-3
PWY-5850 4.22e-3
PWY-5896 4.22e-3
PWY-5845 4.52e-3
PWY-5177 5.81e-4
PWY-841 0.024
PWY0-162 5.40e-3
GLUTORN-PWY 0.038
PWY-7315 2.27e-3
PWY-5920 0.042
PWY-6562 0.016
PYRIDOXSYN-PWY 0.025
P461-PWY 0.012
PWY-5860 6.75e-3
PWY-5862 7.08e-3
PWY-2942 0.015
GLUCUROCAT-PWY 0.013
GLYCOLYSIS 2.16e-3
ECASYN-PWY 3.26e-3
PWY-7196 3.05e-3
AST-PWY 0.041
PWY-7237 0.035
PWY-5747 0.034
GALACTUROCAT-PWY 0.020
ANAEROFRUCAT-PWY 0.041
PWY-5347 3.59e-3
GLYCOL-GLYOXDEG-PWY 0.022
CALVIN-PWY 0.039
PWY0-1533 0.016
GALACT-GLUCUROCAT-PWY 0.026
ORNARGDEG-PWY 0.032
ARGDEG-PWY 0.032
PWY0-321 0.033
PWY-6071 0.033
ORNDEG-PWY 0.031
PROTOCATECHUATE-ORTHO-CLEAVAGE-PWY 0.041
3-HYDROXYPHENYLACETATE-DEGRADATION-PWY 0.036
PWY-6383 0.025
P562-PWY 0.023
GLUCARDEG-PWY 0.034
GLUCARGALACTSUPER-PWY 0.035
GALACTARDEG-PWY 0.035
PWY0-1338 0.035
PWY-7094 0.034
PWY-5677 3.59e-3
PWY0-41 0.021
PWY-5705 0.019
THREOCAT-PWY 0.034
PWY-5088 2.76e-3
PWY1G-0 0.030
p-value (corrected)
0.0 0.9
Mean proportion (%)
−0.20 −0.15 −0.10 −0.05 0.00 0.05 0.10 0.15 0.20 0.25
Difference in mean proportions (%)

b

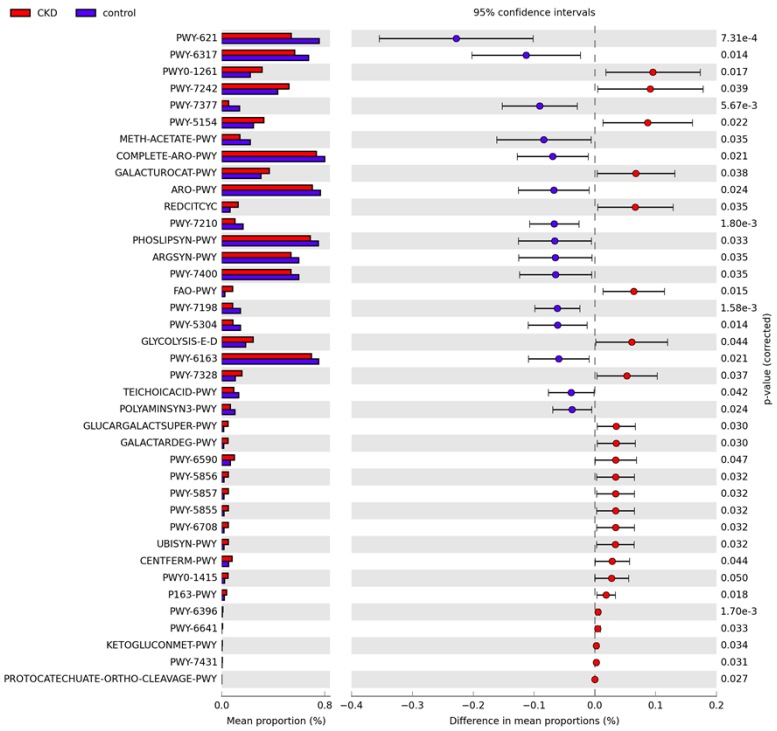
CKD
control
95% confidence intervals
PWY-621 7.31e-4
PWY-6317 0.014
PWY0-1261 0.017
PWY-7242 0.039
PWY-7377 5.67e-3
PWY-5154 0.022
METH-ACETATE-PWY 0.035
COMPLETE-ARO-PWY 0.021
GALACTUROCAT-PWY 0.038
ARO-PWY 0.024
REDCITCYC 0.035
PWY-7210 1.80e-3
PHOSLIPSYN-PWY 0.033
ARGSYN-PWY 0.035
PWY-7400 0.035
FAO-PWY 0.015
PWY-7198 1.58e-3
PWY-5304 0.014
GLYCOLYSIS-E-D 0.044
PWY-6163 0.021
PWY-7328 0.037
TEICHOICACID-PWY 0.042
POLYAMINSYN3-PWY 0.024
GLUCARGALACTSUPER-PWY 0.030
GALACTARDEG-PWY 0.030
PWY-6590 0.047
PWY-5856 0.032
PWY-5857 0.032
PWY-5855 0.032
PWY-6708 0.032
UBISYN-PWY 0.032
CENTFERM-PWY 0.044
PWY0-1415 0.050
P163-PWY 0.018
PWY-6396 1.70e-3
PWY-6641 0.033
KETOGLUCONMET-PWY 0.034
PWY-7431 0.031
PROTOCATECHUATE-ORTHO-CLEAVAGE-PWY 0.027
p-value (corrected)
0.0 0.8
Mean proportion (%)
−0.4 −0.3 −0.2 −0.1 0.0 0.1 0.2
Difference in mean proportions (%)

a

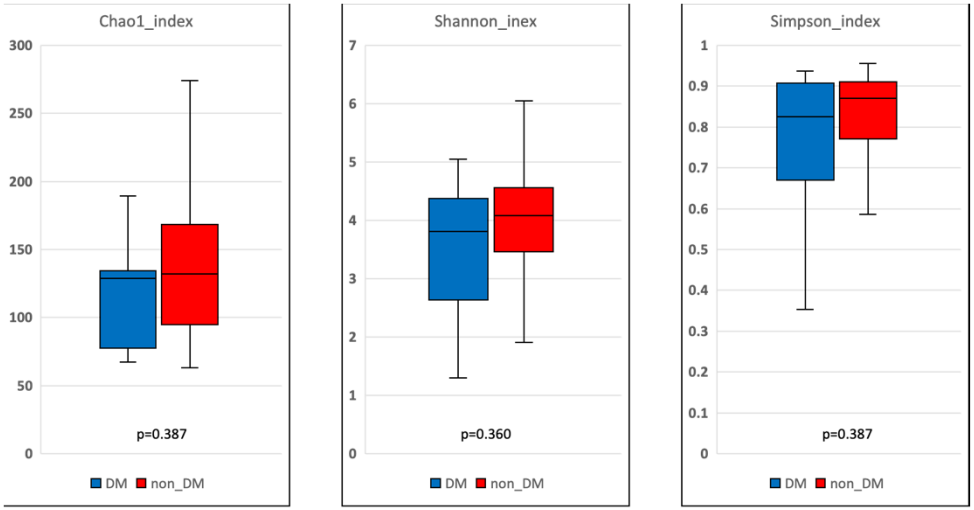
Chao1_index
300
250
200
150
100
50
0
p=0.387
DM non_DM
Shannon_inex
7
6
5
4
3
2
1
0
p=0.360
DM non_DM
Simpson_index
1
0.9
0.8
0.7
0.6
0.5
0.4
0.3
0.2
0.1
0
p=0.387
DM non_DM

b

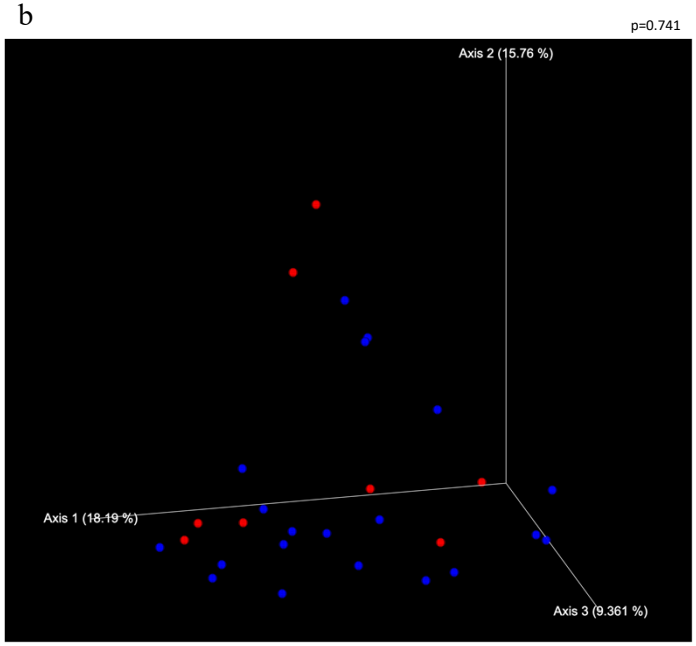
p=0.741
Axis 2 (15.76 %)
Axis 1 (18.19 %)
Axis 3 (9.361 %)

a

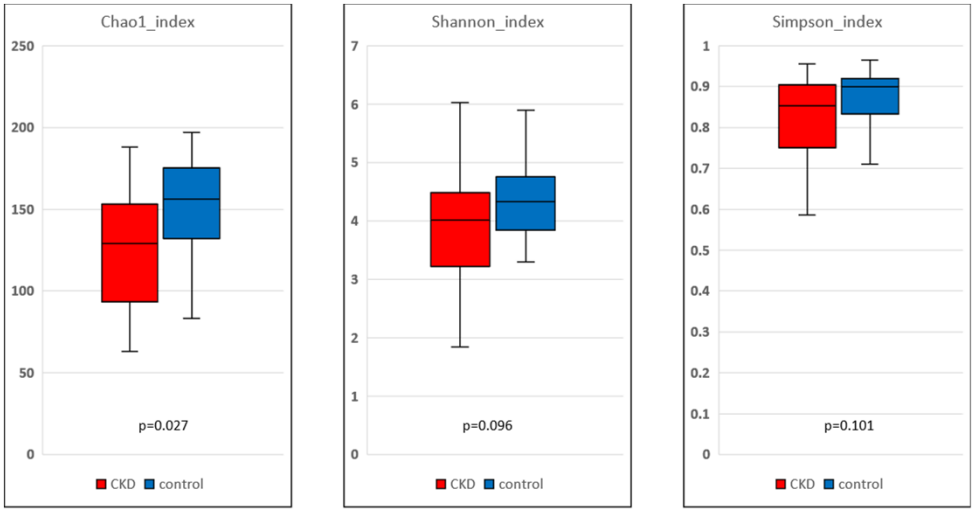
Chao1_index
250
200
150
100
50
0
p=0.027
CKD control
Shannon_index
7
6
5
4
3
2
1
0
p=0.096
CKD control
Simpson_index
1
0.9
0.8
0.7
0.6
0.5
0.4
0.3
0.2
0.1
0
p=0.101
CKD control

b

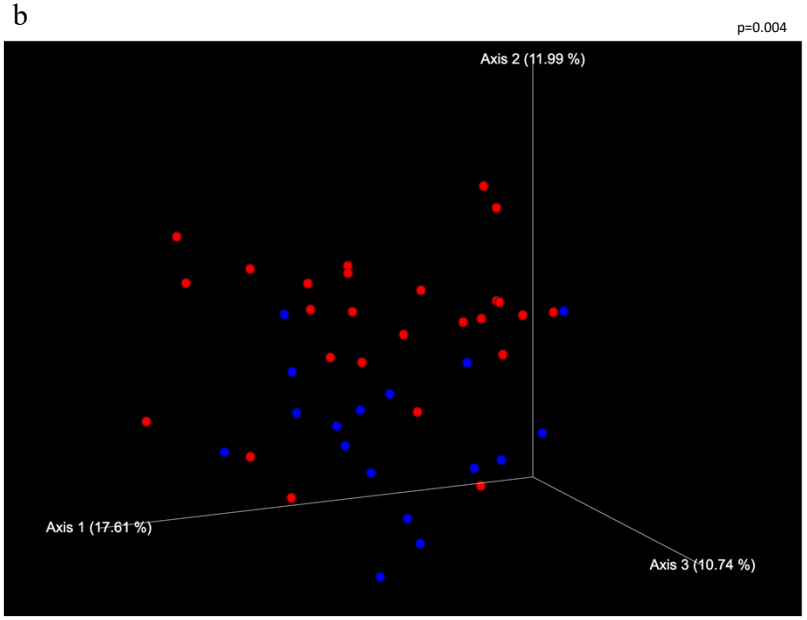
p=0.004
Axis 2 (11.99 %)
Axis 1 (17.61 %)
Axis 3 (10.74 %)